NMR study of copper with vanadium impurities*

D. M. Follstaedt[†] and C. P. Slichter

Materials Research Laboratory, University of Illinois, Urbana, Illinois 61801

(Received 22 February 1977)

We present NMR data on copper with dilute vanadium impurities. We have measured the Knight shift of the ^{51}V impurity resonance and analyzed it in terms of a nonmagnetic virtual bound state. We have detected several host satellite resonances. One has a very large quadrupole coupling constant $\nu_Q \sim 3.5$ MHz and asymmetry parameter $\eta \sim 0.3$; we identify it as the first-neighbor resonance. A magnetic satellite with shift $\Delta K/K = -0.658 \pm 0.015$ is thought to be the resonance of the second or fourth neighbors. A satellite with weak magnetic coupling $\Delta K/K = +0.2 \pm 0.1$ is probably due to third neighbors. Our studies conclude that vanadium impurities in copper are magnetically similar to cobalt impurities.

I. INTRODUCTION

When iron group transition elements are placed as impurities in copper, a very wide range of values for the impurity magnetization is observed.[1] The elements near the center of the group, Cr, Mn, and Fe, have moments comparable to those in ionic solids and have a temperature-dependent susceptibility. The initial and final elements, Sc, Ti, and Ni, have a weaker Pauli-like temperature-independent susceptibility. Co impurities have a weak temperature dependence and thus appear to lie between these two limits. As we shall demonstrate, V impurities are similar to Co.

NMR spectroscopy of both impurity and host nuclei has been shown to be a useful tool to study such impurities. The impurity Knight shift contains components proportional to both the impurity orbital and spin susceptibilities.[2] Their values give estimates of the parameters of the $3d$ impurity electron states. We have observed the ^{51}V impurity resonance in copper and present the analysis in Sec. II.

Host nuclei which are near neighbors to the impurity can have their nuclear resonance frequency significantly perturbed by the impurity. Magnetic shifts from the pure-copper frequency are proportional to the impurity spin susceptibility and reflect its temperature dependence.[3,4] However, even more information is available from satellite shifts. Since near-neighbor nuclear positions satisfy $k_F r \sim 1$, the satellite shifts are determined by conduction electron scattering below the Fermi energy, E_F. Thus detailed knowledge of satellite shifts at near-neighbor sites can in principle be used to completely describe conduction-electron scattering by the impurity site, but we lack data on enough satellites to do so for CuV. Our CuV satellite spectra are discussed in Sec. III.

The above two types of measurements do not involve precise knowledge of the concentration of dissolved isolated impurities. They are thus especially valuable in a poor metallurgical system like CuV where the impurities are nearly insoluble. A third type of NMR measurement, magnetic broadening of the "bulk" resonance of distant host nuclei by the impurity moment, does involve knowing this concentration. We report our observed broadening in Sec. III E, but accept the results with reservations. Conclusions from our results are given in Sec. IV.

Finally, we note that observation of weak impurity and satellite resonances requires a high-sensitivity NMR spectrometer, especially to detect the very weak first-order quadrupole satellites. We have used a hybrid-junction continuous-wave spectrometer. The merits of this spectrometer for satellite detection have been previously discussed along with its components.[5] Details of construction for long-term stability are given elsewhere.[6]

II. VANADIUM RESONANCES

We discuss below two ^{51}V resonances: that of isolated impurities in copper and that of undissolved vanadium metal remaining in our samples. By considering the intensities of both resonances we are able to estimate the dissolved vanadium in our samples. The temperature dependence of the dissolved ^{51}V Knight shift allows us to deduce microscopic parameters of vanadium impurities in copper.

Although the ^{51}V frequency is similar to that of ^{63}Cu (11.193 MHz/10 kG and 11.285 MHz/10 kG, respectively), we can distinguish ^{51}V resonances from ^{63}Cu satellites by the absence of such a resonance in the ^{65}Cu spectrum (12.090 MHz/10 kG).

A. CuV samples

Samples were formed by arc melting high-purity (99.999%) copper with small amounts of vanadium

(99.98%) in an argon atmosphere. Upon termination of the arc, the ingot cools rapidly on the water-cooled copper hearth of the furnace. This hopefully quenches the nearly insoluble vanadium as impurities in the copper host with a solubility more characteristic of molten copper[7] (a few tenths atomic percent). Chemical analysis of the three samples used in this study gave the following average concentrations: 0.045±0.003, 0.275 ±0.005, and 0.173±0.012 at.%, where the variations were obtained by analyzing at least two different portions of the ingot. These are the total vanadium concentrations, whatever the form of the vanadium. Mass spectrography analysis showed less than 12 ppm (within a factor of 3) total concentration of other $3d$ elements and less than 50 ppm of all other elements.

The ingots were filed with a tungsten-carbide rotary cutter to obtain 325- and 400-mesh powders.

B. Estimated dissolved concentrations

Shown in Fig. 1 are the two ^{51}V resonances observed in the 0.275-at.% sample at 4.2 K, 9.3 kG. The resonance closest to the main line is that of pure vanadium metal as is evident from its Knight shift of 0.56%. The second resonance is due to dissolved vanadium and has a Knight shift of 0.14 ±0.02% at 4.2 K. This value agrees well with that of Boyce[8] obtained with a pulsed spin-echo double-
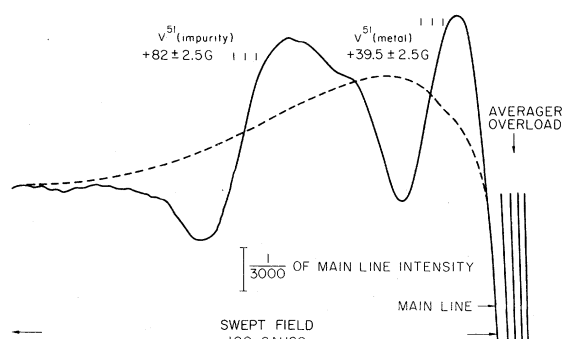

FIG. 1. ^{51}V resonances on the high-field side of the ^{63}Cu main line, obtained with the 0.275-at.% sample at 4.2 K and 10.5 MHz (9.281 KG). The resonance nearest the main line is due to undissolved vanadium metal; the second is due to vanadium impurities in copper. This spectrum was obtained by digitally storing and averaging 64 sweeps of this region of field (requiring $\sim 1\frac{1}{4}$ h) with a 1-sec lock-in time constant and a modulation of ~ 2.5 G at 150 Hz. The dashed line is the estimated ^{63}Cu baseline, giving the resonance positions indicated. The center position and limits of error (e.g., 10 G) are indicated by short vertical bars for each satellite in this and other figures.

resonance (SEDOR) experiment. The SEDOR experiment supports our identification of this resonance as that of ^{51}V impurities dissolved in copper since in SEDOR one observes the effect on the vanadium echo of a pulse tuned to copper nuclei.

These two resonances were also observed at 55 kG, 300 K, where they are completely resolved from the ^{63}Cu resonance. By comparing the intensity of the impurity resonance with the ^{63}Cu main line, we estimate the dissolved concentration to be $c \sim 0.13$ at.% (correcting for modulation effects and assuming complete wipeout of the noncentral transition of both ^{51}V and ^{63}Cu nuclei). This value is supported by the intensity ratio of undissolved to dissolved ^{51}V (~ 1.2) when considered with the total vanadium concentration.

The ^{51}V resonances were observed in the 0.045-at.% sample only at 4.2 K, 9.3 kG, where the metal resonance is difficult to resolve from the ^{63}Cu resonance. We have corrected its intensity with the ratio by which this resonance appeared to increase in the 0.275-at.% sample when it was completely resolved at 55 kG. We can then estimate the dissolved concentration to be $c \sim 0.03$ at.%.

Our detection of undissolved vanadium points up a problem in interpreting the results of bulk measurements on CuV. For instance, Brewig et al.[9] find discrepancies in fitting their bulk experimental data on Ti and V in Cu to a nonmagnetic virtual bound-state model.[10] Their results give 3.0 $3d$ electrons for Ti versus 2.3 for V, whereas from free-atom configurations, more are expected for V. Undissolved vanadium might account for the discrepancy. For instance, their residual resistivity (~ 6 $\mu\Omega$ cm/at.%) allows only 1.9 $3d$ electrons in a virtual bound state. The presence of undissolved vanadium would make a larger resistivity value more appropriate, requiring more $3d$ electrons, in closer agreement with the expected trend.

C. Temperature dependence of the impurity Knight shift

In addition to the work at 4.2 K, the impurity Knight shift was also measured at 300 K, 55 kG, and found to be 0.202±0.005%. The temperature dependence enables us to deduce the spin and orbital contributions to the magnetic susceptibility.

The analysis of impurity Knight shifts with a Hartree-Fock model has been given by Narath.[2] The shift has three contributions:

$$K = K^{\text{cond}} + K^{\text{spin}} + K^{\text{orb}}. \tag{1}$$

The first is that due to the contact interaction of conduction electrons [$\sim (0.1-0.2)$%]. The other two are due to the spin and orbital impurity moments, and are related to their respective susceptibilities by

$$K^{(i)} = \mu_B^{-1} H_{hfs}^{(i)} \chi^{(i)} , \qquad (2)$$

where $H_{hfs}^{(i)}$ is the hyperfine coupling constant and μ_B the Bohr magneton. χ^{orb} is temperature independent so that all temperature dependence is in χ^{spin}.

We shall show below (Sec. III C) that χ^{spin} changes by ~7% between 4.2 and 300 K. This and our observed change in Knight shift then require $K^{spin} \approx -K^{orb} \approx -1.0\%$. The hyperfine coupling constants are estimated to be $H_{hfs}^{spin} \approx -100$ kG$/\mu_B$ and $H_{hfs}^{orb} \approx +200$ kG$/\mu_B$ for vanadium. These values give $\chi^{spin} = 2\chi^{orb} = 1.0 \times 10^{-27}$ emu/atom, or a total susceptibility of 1.5×10^{-27} emu/atom. This value agrees with that for CuV obtained by Weiss[11]; however, since we can only estimate the $H_{hfs}^{(i)}$ and since the measured susceptibility may have been influenced by undissolved vanadium, we accept these numbers with caution.

The nonmagnetic virtual bound-state expressions for the susceptibilities are[12,13]

$$\chi^{orb} = 4\rho_d \mu_B^2 , \qquad (3)$$

$$\chi^{spin} = 2\rho_d \mu_B^2 \xi , \qquad (4)$$

where ρ_d is the d-electron density of states for one spin at the Fermi surface. ξ is an enhancement factor of the spin susceptibility due to Coulomb repulsion and exchange between the d electrons. The orbital susceptibility is thought to have less enhancement; we shall neglect it. If we assume these expressions are valid for CuV, our estimates of χ then give $\rho_d = 2.3$/eV atom and $\xi = 4$. This value for ρ_d can be obtained from a nonmagnetic virtual bound state with 3–4 $3d$ electrons and a width of ~1 eV. The enhancement seems reasonable for a weakly magnetic system like CuV.

Finally, we note that comparison of vanadium shifts in the host series Al, Cu, Au gives[14,15] -0.4, -1.0, -3.2% for K^{spin} ($T \approx 0$) and $+0.70$, $+1.0$, $+1.6\%$ for K^{orb}. These trends support an increase in χ across this host series as has been noted for $3d$ impurities.[1]

III. HOST NUCLEAR SPECTRUM

A. General form of host spectrum

For a sufficiently dilute copper-$3d$ transition impurity alloy, the host ^{63}Cu and ^{65}Cu spectra contain a large resonance termed the "main line" due to the "bulk" of the host nuclei which are distant from the impurities. Their nuclear frequencies are not significantly different from those of nuclei in pure copper metal. On the other hand, near neighbor nuclei to an impurity can be significantly perturbed by it and may be detectable as "satellite" resonances shifted outside the main line.[3–5] Two interactions are responsible for their shifts.

First, the magnetic impurity induces an oscillatory magnetization in the surrounding host conduction electrons which is proportional to the time-average impurity spin moment. Neighboring host nuclei are perturbed by their magnetic hyperfine interaction with the magnetization at their site, and thus have an additional magnetic shift (ΔK) as well as the pure copper Knight shift (K). This magnetization will also broaden the main line. Second, since both ^{63}Cu and ^{65}Cu nuclei have $I = \frac{3}{2}$, they have electric quadrupole moments[16] ($^{63}Q = -0.157 \times 10^{-24}$ cm^2 and $^{65}Q = -0.145 \times 10^{-24}$ cm^2) and are perturbed by electric field gradients (efg) in the vicinity of the impurity[17]:

$$\mathcal{H}_Q = [e^2 Qq/4I(2I-1)][(3I_z^2 - I^2) + \eta(I_x^2 - I_y^2)] . \qquad (5)$$

In the quadrupole Hamiltonian $\mathcal{H}_Q$, q is the largest component of the efg tensor and η the asymmetry parameter. Either or both interactions may produce a resolvable satellite resonance for a given neighboring shell of crystallographically identical host nuclei, which can be characterized by ΔK, q, and η.

Perturbation of the nuclear frequency by (5) is dependent upon the orientation of the efg tensor axes (x, y, z) with respect to the external magnetic field $\vec{H}$. For the powdered samples of this study, all orientations are present. The frequency distributions or "powder patterns" of (5) have been determined treating it as a first-order and also as a second-order perturbation on the nuclear Zeeman interaction. The results show nuclear intensity singularities which may be detectable.[18–20] (In this study we may ignore magnetic anisotropies.)

The splitting (ΔH) of such singularities from the main line has the following general field dependence:

$$\Delta H = aH + b + c/H . \qquad (6)$$

aH is the magnetic splitting, and b and c/H are first-order and second-order quadrupole splittings, respectively. If a detected satellite is due to the central ($\frac{1}{2} \leftrightarrow \frac{1}{2}$) transition of a near-neighbor nucleus, it will necessarily have $b = 0$ since first-order perturbation results give no shift of this transition.[17] Intensity considerations of satellites due to noncentral ($\pm\frac{3}{2} \leftrightarrow \pm\frac{1}{2}$) transitions for which b is measurable require a small q ($b \propto q$) and thus c/H is not detectable ($c \propto q^2$). Satellites which are central transitions of neighbors with a large q may be detectable as c/H field-dependent singularities. Either or both types of quadrupole satellites may or may not have a superimposed magnetic field dependence aH. Finally, we may have a magnetic satellite with no measurable quadrupole interactions.
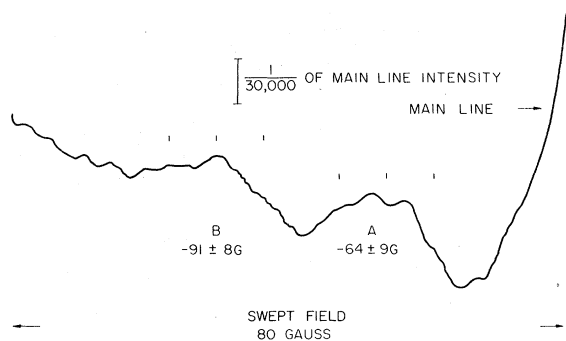
In the spectra to be discussed below we will en-

D. M. FOLLSTAEDT AND C. P. SLICHTER

FIG. 2. Satellites A and B on the low-field side of the ^{63}Cu main line, obtained with the 0.045-at.% sample at 4.2 K and 7.9 MHz (6.984 KG). This spectrum was obtained after averaging 422 sweeps (~ 8 h) with a 1-sec lock-in time constant and a modulation of ~5 G.

counter four first-order quadrupole satellites with $b \neq 0$ (one of which has $aH \neq 0$), one second-order quadrupole satellite with $c/H \neq 0$, and one purely magnetic satellite with $aH \neq 0$.

B. Low-field satellite spectrum

Data presented in this section were obtained with $H \lesssim 10$ kG at 4.2 K. ^{63}Cu satellites detected on the low-field side of the main line are shown in Figs. 2 and 3, labeled $A-F$. The smaller ones (B, D, E, and F) required extensive signal averaging to detect. The field dependence of the spectrum of the 0.045-at.% sample is shown in Fig. 4. The larger ^{51}V resonances are included to show the portion of the ^{63}Cu spectrum which they obscure.

1. Satellites A, B, C, and E

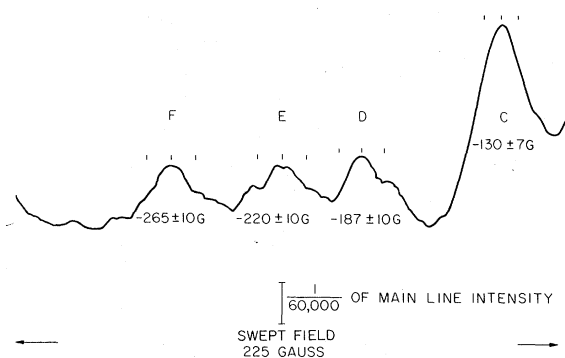These satellites have field-independent splittings over a factor of two in field (5–10 kG). We also

FIG. 3. Satellites C, D, E, and F on the low-field side of the ^{63}Cu main line, obtained with the 0.045-at.% sample at 4.2 K, 11.26 MHz (9.951 KG). This spectrum was obtained by averaging 537 sweeps (~ 10 h) with a 1-sec lock-in time constant and a modulation of ~14 G.

find lines on the high-field side of the main line (labeled with primes) with the same field-independent splittings and intensity. This is required for a first-order quadrupole satellite because the frequency shifts of the $(+\frac{3}{2} \leftrightarrow +\frac{1}{2})$ and $(-\frac{3}{2} \leftrightarrow -\frac{1}{2})$ transitions are equal in magnitude but opposite in sign.

We have observed four corresponding field-independent lines in the ^{65}Cu spectrum. The ratio of their splittings to those indicated in Fig. 4 is 0.87 ±0.06, compared with the expected ratio $(^{63}\gamma/ ^{65}\gamma) {}^{65}Q/^{63}Q = 0.86$ for a first-order quadrupole splitting.

This same first-order quadrupole spectrum was observed in the 0.275-at.% sample, establishing the concentration independence of the splittings. However, the increased vanadium impurity concentration did not increase the satellite intensities. Taking account of first-order quadrupole wipeout, the intensity should go with concentration as

$$I \propto c(1-c)^n \approx c(1-nc), \tag{7}$$

which peaks at $c \sim \frac{1}{2}n$, where n is the wipeout number. Typically, $n \sim 1000$, so the optimum concentration is ~0.05 at.%. The estimated dissolved vanadium concentrations of our two samples (see Sec. II B) are a factor of ~2 on either side of this value, and thus are predicted to have similar in-
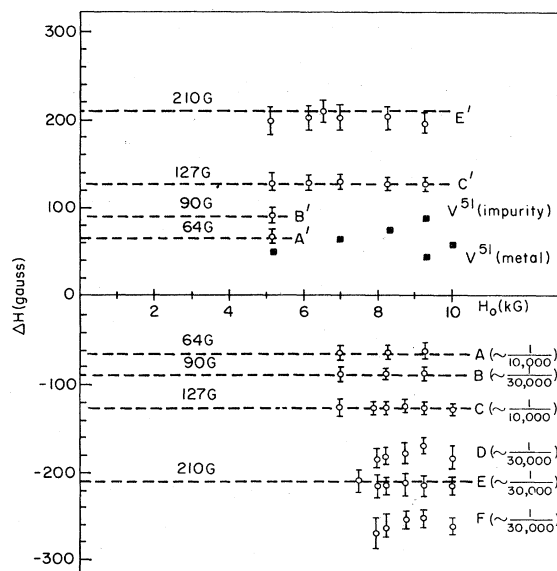

FIG. 4. ^{63}Cu satellite splittings obtained with the 0.045-at.% sample at 4.2 K for fields less than 10 KG. Satellites on the high-(low-) field side of the main line are plotted with positive (negative) ΔH values versus applied field. Intensities of the low-field satellites with respect to the main line are given in parentheses. Also shown are the positions of the two vanadium resonances.

TABLE I. ^{63}CuV satellite parameters.

Satellite	η	ν	q (10^{22} cm^{-3})	$-\Delta K/K$ ($T \sim 0$)	Shell
A	~0	144 ± 11 kHz	5.30 ± 0.40		
B	~0	203 ± 11 kHz	7.45 ± 0.40		
C	~0	287 ± 7 kHz	10.50 ± 0.25	+ 0.2 ± 0.1	3 ?
E	~0	475 ± 16 kHz	17.1 ± 0.6		
D and F	~0.3	~3.5 Mhz	~128		1
G				−0.658 ± 0.015	2 (or 4 ?)

tensities just as we observe.

The high-field spectrum to be discussed below (Sec. III C) shows that A and C are due to different neighboring shells. We shall therefore interpret A, B, C, and E as being singularities of powder patterns of four different shells. For quadrupole couplings with $\eta \approx 0$, the patterns[19] are dominated by one singularity at $\Delta H = \pm \pi \nu_Q / \gamma$, where the quadrupole frequency is defined as $\nu_Q \equiv 3e^2 Qq/2I - 1)\hbar$. Using this interpretation gives the quadrupole parameters listed in Table I. (Intensity considerations[19] show that it is also possible that B and E are both due to a single shell with two singularities and $\eta \neq 0$. This interpretation gives $\eta = 0.43 \pm 0.06$, $\nu_Q = 331 \pm 12$ kHz, and $q = 1.19 \pm 0.04 \times 10^{23}$ cm^{-3}.)

2. Satellites D and F

These satellites differ from the above in that no corresponding lines are found on the opposite side of the main line. The splittings appear to be larger for lower magnetic fields. Unfortunately, we were unable to go below 8 kG due to interference from the ^{65}Cu spectrum. Thus spectra with the iron core magnet were obtained only between 8–10 kG, where the field dependence is not accurately discernible. The low intensities and difficulty of resolution from E evidently prevent observation of corresponding resonances on the low-field side of the ^{65}Cu spectrum. ^{65}Cu also offers less sensitivity than ^{63}Cu as it is not as isotopically abundant (30% vs 70%).

D and F lie on either side of a CuV satellite detected by Boyce in the SEDOR experiment.[8] His ^{63}Cu satellite splittings are plotted against H_0^{-1} along with those of D and F in Fig. 5. The SEDOR splittings indicate a H_0^{-1} dependence, albeit over a limited field range. However, the satellite was also detected with ^{65}Cu nuclei, and the splittings scaled as $(^{65}Q/^{63}Q)^2$, thus also indicating a second-order quadrupole perturbation.

On the basis of the above, we conclude that D and F are the same satellite as detected in the SEDOR experiment. SEDOR powder patterns have been shown to be different from those of continuous-

wave[8] NMR: thus D or F are not to be expected to agree identically with the SEDOR satellite position. Furthermore, the SEDOR satellite is roughly as wide as the splitting between D and F and thus cannot exhibit the more detailed structure we are detecting.

For $\eta \neq 0$, Baughier et al.[20] have shown that the low-field side of the second-order powder pattern for the ($\frac{1}{2} \leftrightarrow -\frac{1}{2}$) transition has two singularities of comparable intensities. Neglecting possible magnetic shifts, the singularities we detect at 8.8 kG can be fit with $\nu_Q \sim 3.5$ MHz and $\eta \sim 0.3$. There are also high-field singularities in the powder pattern which we evidently cannot detect. Probably their weak intensities (comparable to or less than that of D) do not permit detection in the midst of the larger high-field satellite C' and the vanadium resonances.
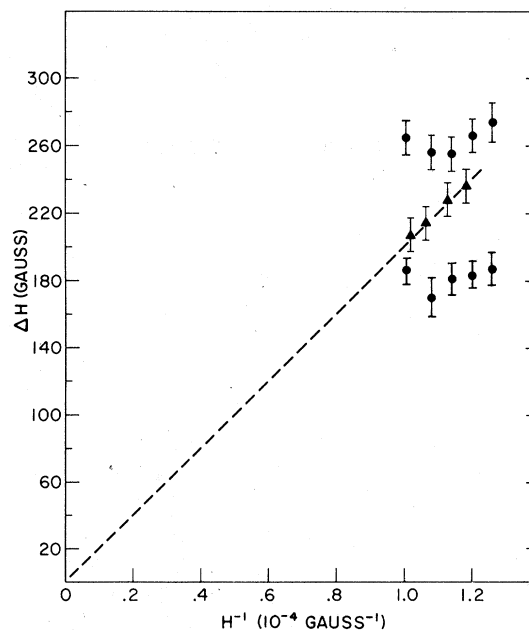

FIG. 5. Splittings of satellites D and F and the SEDOR satellite plotted vs H^{-1}. SEDOR splittings were obtained from Ref. 8.

C. High-field satellite spectrum

Shown in Fig. 6 are the splittings of three satellites observed between 15–55 kG at 300 K in the 0.275-at.% sample. For completeness, the positions of the ^{51}V resonances are also indicated.

1. First order quadrupole satellites

We begin with the two satellites on the low-field side of the main line. The closest satellite has a field-independent splitting of -69 ± 4 G. Its position and intensity are essentially the same as satellite A in the low-field spectrum at 4.2 K (Fig. 5), and we take them to be the same resonance.

The larger split low-field satellite is a first-order satellite with a weak magnetic splitting. Its zero-field intercept gives -112 ± 10 G, and it has a magnetic shift relative to the pure-copper Knight shift of $\Delta K/K \approx +0.2 \pm 0.1$. Its intensity is about the same as C in the low-field spectrum, with its zero-field intercept differing by $\sim -10\%$ from the splitting of C. Quadrupole couplings of the satellites might be expected to be temperature independent but this small change does not appear unreasonable, and the identification with C is too obvious to overlook. The small magnetic shift would not have been observable for $H < 10$ kG.

2. Magnetic satellite

The high-field satellite G shown in Fig. 7 is detectable at high fields, disappearing into the main line for $H < 30$ kG. Its splitting has a purely linear field dependence described by $\Delta K/K = -0.616 \pm 0.009$. This shift and its larger relative intensity show that G is a different resonance from any of the first-order quadrupole satellites. The size of
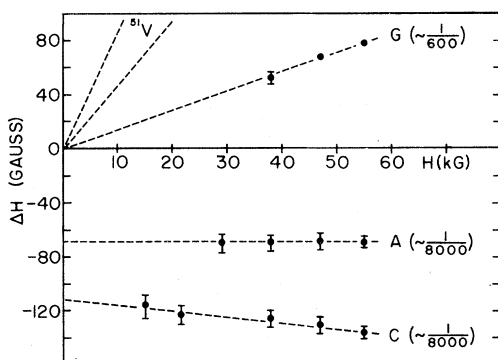

FIG. 6. ^{63}Cu satellite splittings obtained with the 0.275-at.% sample at 300 K plotted vs applied field (up to 55 KG). Relative intensities are shown in parentheses. The positions of the ^{51}V resonances are indicated to show the portion of the ^{63}Cu spectrum which they obscure.

the quadrupole coupling estimated for D and F would require a noticeable c/H dependence in the splitting of G, which is absent. Thus G is a resonance from a different neighboring shell.

The splitting of G was also measured at 4.2 and 1.5 K ($H = 58$ kG) and found to be $\Delta K/K = -0.658 \pm 0.015$. Thus we measure a 7% change in χ^{spin} between 1.5 and 300 K. Two temperature dependences are accepted for Kondo impurities[21]:

$$\chi^{\text{spin}} \propto 1/(T + T_K) \quad (T \gtrsim T), \tag{8}$$

$$\chi^{\text{spin}} \propto 1 - (T/T_K)^2 \quad (T \ll T_K). \tag{9}$$

Our change in $\Delta K/K$ can be accounted for by using $T_K = 4300 \pm 1900$ K in the Curie-Weiss formula (8) or by $T_K = 1600 \pm 290$ K in the quadratic formula (9). Since $300 \ll 4300$K, the weaker quadratic temperature dependence appears more plausible although we cannot experimentally verify this.

3. Unobserved resonances

The unobserved high-field satellites corresponding to A and C in Fig. 6 are easily explained by their overlap with the much larger satellite G and the ^{51}V resonances. At 300 K, the sensitivity with 55 kG is not as good as at 4.2 K with 10 kG. Thus the weak resonances B and E are not observed.

Although D and F are very weak at 10 kG, the intensity of a second-order powder pattern is expected to increase at high fields as the pattern width decreases. However, the estimated quadrupole coupling is large enough to produce a pattern ~ 100 G wide at 50 kG. Its singularities would be weaker than satellite G or the ^{51}V resonances, and thus any singularities on the high-field side of the main line (where the quadrupole splitting is largest) could go undetected. Scaling the splittings of D and F as H^{-1} to 55 kG gives a splitting of ~ -40 G, where they should have an intensity comparable to A. If the pattern had a magnetic shift strong enough to shift the singularity out to the position of A, we might expect to be able to detect it. If, however, $\Delta K/K < +0.25$, the D–F singularity could be too close to the main line to detect. Such conclusions drawn on the absence of a resonance should be regarded as very speculative, however.

Other magnetic satellites might have been expected to split from the main line at high fields provided their magnetic coupling is strong enough. A reasonable upper limit on the undetected splittings is $|\Delta K/K| \lesssim 0.3$.

D. Identification of satellite shells

We begin with the shell identification of satellites D, F, the SEDOR satellite G, and C. These have distinguishing features which are clues to

their identity. We can only guess at the identity of other satellite shells.

1. Satellites D, F, and SEDOR

The quadrupole frequency we have estimated is larger than any observed in other copper alloy systems (see Table I of Ref. 22) and thus requires a very-near-neighbor assignment. The nonzero η rules out the second-neighbor shell (for which $\eta = 0$ by symmetry), and ν_Q is much too large to make a more distant shell plausible. Furthermore, the SEDOR technique is sensitive to very near neighbors[8]; a CuCo SEDOR satellite has been identified as the first-neighbor resonance with a single crystal rotation study.[23] Thus, we feel confident in assigning these satellites to the first-neighbor shell.

2. Satellite G

Using intensity measurements to identify satellites is usually questionable because of the unknown concentration of isolated impurity atoms. Fortunately, in this case the ^{51}V impurity resonance intensity (Sec. II B) shows that $c_{\text{isol.}} \approx 0.13$ at.%. This value predicts satellite intensities (relative to the main line) of $\sim\frac{1}{140}$, $\sim\frac{1}{35}$, and $\sim\frac{1}{70}$ for the second-, third-, and fourth-neighboring shells, respectively. The second neighbor is closest to the observed intensity $(\frac{1}{600})$ which is possibly diminished by the tail of the main line.

Shown in Fig. 7 is a plot of magnetic satellite shifts divided by the impurity susceptibility for iron-group impurities in copper (see Ref. 22 for references on $\Delta K/K$ and χ). Since the conduction-electron magnetization is proportional to χ, such a plot allows us to compare the shifts of adjacent impurities without the large variation in magnitude between the ends and middle of the group. The identified satellite shells show that $\Delta K/K\chi$ for a particular shell does not have a random behavior in crossing the iron group, but rather exhibits trends. The first-neighbor trends of Fe, Mn, and Cr, suggest that G could also be a first neighbor, but we have ruled this out. A second-neighbor trend from Fe and Mn passing through $\Delta K/K \approx 0$ at Cr, and then to the Ti satellite would account for G. It is also possible that the fourth-neighbor trend from Mn and Cr dips at V and is undetected in Ti. Other shells seem much less probable. Thus G is likely the second neighbor, though the fourth is not ruled out.

3. Satellite C

The $\Delta K/K$ trend for the third neighbor in Fig. 7 from Mn to Cr gives fair agreement with C. No other shell trends are clearly indicated for the

position of C. However, other shells with $\Delta K/K > 0$ but not as widely split as the third in Mn and Cr might be possible.

4. Satellites A, B, and E

Little can be said about the identification of A, B, and E, except that they are probably more distant than the third shell. Likely near-neighbor candidates (and their number of shell members) are the fourth (12), fifth (24), seventh (48), and ninth (36). Since A has the largest intensity, we might speculate that it is perhaps the seventh neighbor.

E. ^{63}Cu main linewidth

The ^{63}Cu main linewidth was measured to be 8.5 ±0.4 G (peak to peak) at 55 kG, 300 K, for the 0.275-at.% sample and was found to decrease to the pure-copper dipole-dipole linewidth of 6.5 G at lower fields. The measured linewidth is a convolution of the pure-copper line shape and a magnetic broadening line shape due to the oscillatory conduction-electron magnetization induced by distant impurities. Assuming the magnetic line shape is Lorentzian, we can use the results of Sugawara[24] to deconvolute the measured linewidth, obtaining a full magnetic width of $\sim$4.5 G.

This width can be analyzed with the results of Walstedt and Walker.[25] Assuming the oscillatory magnetization of an isolated impurity goes as

$$H(r) = (A/r^3)\cos(2k_F r + \phi), \tag{10}$$

they compute the half width of the Lorentzian broadening to be

$$\Delta = 16\pi Ac/3a^3 \tag{11}$$

for a fcc lattice with cubic lattice constant a and impurity concentration c. Using an isolated impurity concentration of $c \approx 0.13$ at.%, we obtain $A \approx 5\times10^3$ G Å^3 at 300 K. This value is comparable to the CuCo value for isolated impurities[5] of 6.6 $\times10^3$ G Å^3. However, it is difficult to compare such close values because of the poor metallurgy of the two systems and known clustering in CuCo.

In the Ruderman-Kittle-Kasuya-Yosida theory for these oscillations, $A \propto \chi J$, where J is the impurity exchange constant. Using $\chi^V = 1.5\times10^{-27}$ emu/atom and $\chi^{Co} = 4.0\times10^{-27}$ emu/atom, we obtain $J^V \sim 2J^{Co}$. With the uncertainties in χ, c, and A, it is perhaps wiser to simply say J^V is comparable to or perhaps slightly greater than J^{Co}.

The linewidth was also measured with the 0.173-at.% sample at 58 kG, 4.2 K, and found to be 11.7 ±1.0 G, giving $\sim$9.1 G for the full magnetic width. Generously estimating the dissolved vanadium concentrations for this sample to be $c \lesssim 0.12$ at.%, we obtain $A \gtrsim 10\times10^3$ G Å^3 at 4.2 K. All uncertainties
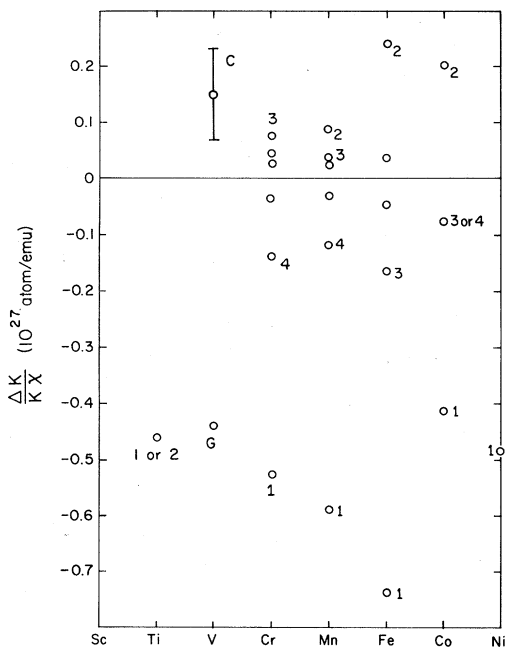
FIG. 7. $\Delta K/K\chi$ for satellites due to iron-group impurities in copper as measured by the University of Illinois NMR group. Numerals for the series Cr-Ni are the numbers of the neighboring shells producing the resonances as determined by single crystal studies (Refs. 23 and 28). Identification of the Ti satellite (Ref. 22) is on the basis of quadrupole parameters ν_Q and η. Additional details are given in Ref. 22.

considered, this value is more than the 7% increase expected from the temperature dependence of $\Delta K/K$. Thus it seems that the low-temperature linewidth is being influenced by the stronger temperature dependence of magnetic impurity clusters, similar to effects observed for $Cu\mathrm{Co}^5$ and $Cu\mathrm{Fe}$ (discussed in Ref. 4).

IV. SUMMARY AND CONCLUSIONS

Our analysis of the ^{51}V impurity resonance places the spin and orbital susceptibilities of CuV between those of AlV and AuV as expected. Analysis of these susceptibilities with a nonmagnetic virtual bound-state model gives a spin susceptibility enhancement of four, which seems reasonable for a weakly magnetic impurity. The width we deduce of the virtual bound state (~1 eV) agrees with expected values. However, use of this model must be regarded as an assumption which could be wrong.

A summary of our satellite couplings is given in Table I along with neighboring shell assignments. First-order quadrupole satellites A, B, and E have magnetic couplings too small to detect. There is a little evidence for their identification, and we

have omitted it. Satellites D, F, and SEDOR have been grouped together as part of a second-order quadrupole powder pattern with a relatively large ν_Q and nonzero η. We are reasonably confident of a first-neighbor shell assignment for the pattern, although this identification cannot be as definite as from a single-crystal study. The magnetic satellite G is probably the second or fourth neighbor, and satellite C, probably the third.

We have mentioned that satellite coupling parameters depend upon conduction-electron scattering beneath the Fermi surface, and can in principle give the details of the scattering. Most of the satellite parameters in CuV are quadrupole couplings. Unfortunately, the current theoretical treatment of quadrupole couplings is not good enough to reveal scattering details. In systems where a large number of magnetic satellites have been identified by single-crystal studies, efforts are underway to model the impurity scattering with a virtual bound state.[26,27] This approach will be difficult for V, Ti, and Sc impurities where the susceptibilities are small and fewer magnetic satellites are observed.

Magnetic splittings in these weakly magnetic systems can, however, be used to observe trends in $\Delta K/K\chi$ for a given neighboring shell as we cross the iron group, as shown in Fig. 7. In particular, we mention Aton's suggestion (see Ref. 22) that the rather abrupt change in $\Delta K/K\chi$ of the first neighbor in going from Co to Fe might be an indication that the $3d$-impurity electrons have gone from a nonmagnetic virtual bound state for Co to a magnetic state for Fe. Clearly, there can be other explantions. Turning to CuV satellite G in Fig. 7 and recalling that it is not the first neighbor, we see that it shows a large change in the trend of any shell $n \geqslant 2$. Thus we might speculate that it signals a return to a nonmagnetic virtual bound state in going from Cr to V.

The temperature dependence of the shift of magnetic satellite G gives $T_K \approx 1160$ K, assuming a quadratic temperature dependence. This weak temperature dependence is almost identical to that of CuCo. From a comparison of satellite splittings, magnetic line broadening, and temperature dependence of the spin susceptibility, we conclude that CuV is very similar to CuCo, although the susceptibility appears to be smaller.

ACKNOWLEDGMENTS

*Research supported in part by the U. S. ERDA Contract No. E(11-1)-1198.

†Present address: Division 51111, Sandia Laboratories, Albuquerque, N. M. 87115.

[1]M. D. Daybell and W. A. Steyert, Rev. Mod. Phys. **40**, 380 (1968).

[2]A. Narath, Crit. Rev. Solid State Sci. **3**, 1 (1972).

[3]D. V. Lang, J. B. Boyce, D. C. Lo, and C. P. Slichter, Phys. Rev. Lett. **29**, 776 (1972); Phys. Rev. B **9**, 3077 (1974).

[4]J. B. Boyce and C. P. Slichter, Phys. Rev. Lett. **32**, 61 (1974).

[5]D. C. Lo, D. V. Lang, J. B. Boyce, and C. P. Slichter, Phys. Rev. B **8**, 973 (1973).

[6]D. Follstaedt, thesis (University of Illinois, 1975) (unpublished).

[7]M. Hansen, *Constitution of Binary Alloys* (McGraw-Hill, New York, 1958); R. P. Elliot, *ibid.*, first supplement (1965); F. A. Shunk, *ibid.*, second supplement (1969).

[8]J. B. Boyce, thesis (University of Illinois, 1972) (unpublished).

[9]E. Brewig, W. Kierpse, U. Schotte, and D. Wagner, J. Phys. Chem. Solids **30**, 483 (1969).

[10]E. Daniel and J. Friedel, in *Proceedings of the Ninth International Conference on Low Temperature Physics*, edited by J. G. Daunt, D. O. Edwards, F. J. Milford, and M. Yaqub (Plenum, New York, 1965), p. 933 (Part B).

[11]W. D. Weiss, Z. Metallk. **58**, 895 (1967).

[12]L. Dworin and A. Narath, Phys. Rev. Lett. **25**, 1287 (1970).

[13]B. Caroli, P. Lederer, and D. Saint-James, Phys. Rev. Lett. **23**, 700 (1969).

[14]A. Narath and H. T. Weaver, Phys. Rev. Lett. **23**, 233 (1969).

[15]A. Narath, Solid State Commun. **10**, 521 (1972).

[16]B. Bleaney, K. D. Bowers, and R. S. Trenam, Proc. R. Soc. A **66**, 410 (1953).

[17]C. P. Slichter, *Principles of Magnetic Resonance* (Harper and Row, New York, 1963).

[18]M. H. Cohen and F. Reif, in *Solid State Physics*, edited by F. Seitz and D. Turnbull (Academic, New York, 1957), Vol. 5.

[19]L. E. Drain, Phys. Rev. B **8**, 3628 (1973).

[20]J. F. Baughier, H. M. Kriz, P. C. Taylor, and P. J. Bray, J. Magn. Res. **3**, 415 (1970).

[21]K. Schotte and U. Schotte, Phys. Rev. B **4**, 2228 (1971).

[22]D. M. Follstaedt, D. Abbas, T. S. Stakelon, and C. P. Slichter, Phys. Rev. B **14**, 47 (1976).

[23]T. S. Stakelon and C. P. Slichter, Phys. Rev. B **14**, 3793 (1976).

[24]T. Sugawara, J. Phys. Soc. Jpn. **14**, 643 (1959).

[25]R. E. Walstedt and L. R. Walker, Phys. Rev. B **9**, 4857 (1974).

[26]J. B. Boyce and C. P. Slichter, Phys. Rev. B **13**, 379 (1976).

[27]D. Cohen (private communication).

[28]T. Aton, thesis (University of Illinois, 1976) (unpublished).